ELSEVIER

Journal of Alloys and Compounds 434–435 (2007) 788–791

Journal of ALLOYS AND COMPOUNDS

www.elsevier.com/locate/jallcom

Photodecomposition of NO by sol–gel TiO_2 catalysts under atmospheric conditions: Effect of the method on the textural and morphologic properties

R. Carrera [a,b], A.L. Vázquez [a,b], E. Arce [a], M. Moran-Pineda [b], S. Castillo [a,b,*]

[a] *Departamento de Ingeniería Metalúrgica, ESIQIE-IPN, AP 75-876, México D.F., Mexico*

[b] *Programa de Ingeniería Molecular, Instituto Mexicano del Petróleo, Eje Lázaro Cárdenas 152, C.P. 07730, México D.F., Mexico*

Available online 17 October 2006

Abstract

Photodecomposition of nitric oxide (NO) in the open air by sol–gel TiO_2 catalysts with different solvents and thermal treatments was studied. The sol–gel TiO_2 catalysts showed high surface areas, rich anatase phases, small particle sizes and bandgap-energy changes. The photoactivity was performed in an insulated chamber with 50 ppm (NO) and a 365-UV light. The sol–gel TiO_2 catalysts (which were activated at 200 and 500 °C and prepared by using two different solvents) showed high NO decomposition under UV light illumination. Taking into account the aforementioned results, these catalysts could be applied for the NO decomposition under atmospheric conditions.

Keywords: Nanostructured titania; Sol–gel method; Anatase; Photodecomposition

1. Introduction

Nanostructured materials offer promising opportunities for improved and tailored properties for application in environmental catalysis [1]. TiO_2 is a very interesting material due to its properties and diverse applications. Currently, TiO_2 is an interesting nanoparticle semiconductor material, especially because of its application in photoassisted reactions in the process of reduction or elimination of water contaminants, and the auto cleaning (anti-bacterial, anti-soot), and more recently in the treatment of contaminant gases present in the air and in medicine [2]. As a catalytic support, TiO_2 has a low surface area ($\approx$40 m^2/g), and the crystalline phase with higher photocatalytic activity with respect to rutile is the anatase due to their energy band structures [3].

The synthesis of nanostructured materials like TiO_2 by wet chemistry routes is a powerful way to obtain reproducible homogeneous samples. The control of stable particle size and crystalline phase obtained by the sol–gel method is one of the most versatile, reproducible procedures to obtain high reactivity, small particles and large surface areas [4,5]. Due to its especial characteristics, TiO_2 can be used in photocatalytic processes, and at the same time, offers alternative applications as films or coverings on a grant variety of surfaces or substrates [6]. Application in oxidation and photocatalytic decomposition of atmospheric contaminants, are mainly focused on its textural and morphological properties, synthesis of nanostructured TiO_2 with a high surface area and a controlled and stable phase composition, with the aim of reaching higher photocatalytic activity at lower temperature and closer to the UV light visible region [7–9].

As for the atmospheric contaminants, it is of strategic importance to control the nitrogen oxides (NOx) coming from the combustion of fossil fuels in a great variety of combustion systems [10]. One way of reducing the NOx under outdoors conditions is by photoassisted reactions with the possibility of controlling simultaneously reactive organic gases (GOR) also known as volatile organic compounds (VOC's) [11]. In this work, TiO_2 powder was produced with particle size from 12 to 7 nm, high surface area (>120 m^2/g), and higher anatase phase purity (>90%), for its evaluation in decomposition and photocatalytic oxidation of NOx in a UV light interval as close as possible to the visible spectrum and if possible in this region (solar light), and with a longer useful life.

2. Experimental

TiO_2 catalysts were prepared by the sol–gel method in a three neck glass reactor at atmospheric pressure. Titanium(IV) isopropoxide was used as

* Corresponding author.
E-mail address: scastill@imp.mx (S. Castillo).

0925-8388/$ – see front matter © 2006 Elsevier B.V. All rights reserved.
doi:10.1016/j.jallcom.2006.08.334

precursor and the hydrolysis was carried out with 2-propanol and ethanol and finally with deionized water. The mixture was kept under reflux and uniform stirring until the gel was formed. In postgelation, the product was dried at 70 °C during 12 h and calcined 6 h at 200 and 500 °C. The sol–gel catalysts were labeled as follows: TiO_2-P-200 °C (prepared with 2-propanol and calcined at 200 °C), TiO_2-P-500 °C (prepared with 2-propanol and calcined at 500 °C), TiO_2-E-200 °C (prepared with ethanol and calcined at 200 °C) and TiO_2-E-500 °C (prepared with ethanol and calcined at 500 °C).

The specific area was determined by the BET method through the nitrogen adsorption isotherms at −196 °C. The volume and pore size distribution were calculated from BET isotherms by the BJH method (Barret, Joyner, Halenda), in a Micrometrics ASAP-2000 equipment. For X-ray diffraction analysis, Siemens 500 was used with an anode copper tube and integrated software and the components of each catalyst were determined. The band gap of forbidden energy was determined through visible ultraviolet spectroscopy. Once the diffuse reflectance spectra were obtained, a numerical method was applied to obtain the E_g values [12]. The particle size of the TiO_2 crystals was obtained with a transmission electronic microscope JEOL 100 (X) STEM with resolution ranging from 2 to 5 Å capable of working at 100 kV.

The catalysts were analyzed in the middle infrared by FT-IR Brucker equipment. The samples were prepared in potassium bromide tablets with an approximate ratio of 10 parts of KBr to 1 of sample. The photoactivity was performed in an insulated chamber with 50 ppm (NO) and 365-UV light. The photocatalytic evaluation of the catalysts decomposing the NO was performed with infrared spectroscopy with IFS66V/s equipment with a MCT detector (Mercury–Tellurium–Cadmium) with high sensibility, resolution of 0.5 cm^{-1} and optic step length of 25 cm.

3. Results and discussion

According to the BET results, the sol–gel catalysts that showed higher surface areas, higher pore volume and less mean pore diameter were the ones that were calcined at 200 °C (TiO_2-P-200 °C and TiO_2-E-200 °C) (Table 1). X-ray analysis of the four sol–gel catalysts showed five characteristic peaks for the anatase phase and in a minor signal for the rutile phase, except for the catalyst that was prepared with ethanol and calcined at 500 °C (TiO_2-E-500 °C), where pure anatase was obtained (Fig. 1). Table 1 shows that through sol–gel method, TiO_2 catalysts with nanometric size were obtained which is fundamental to get a high photocatalytic activity in NO photodecomposition. Among the sol–gel catalysts with small crystal size calcined at 200 °C, the one that showed the smaller size was prepared with ethanol (TiO_2-E-200 °C) (Fig. 2).

According to the method used in this work, the fit-plot-yield-bandgap values could change; this change could be related to Quantum-Size effects through the TiO_2 crystalline phases and particle size [13]. The forbidden-energy band of the commercial TiO_2 anatase phase is 3.2 eV with a particle size of 39 nm. As for the diffuse reflectance spectra for the four sol–gel catalysts, the E_g value varied from 3.05 to 3.95 eV, so, it can be said that the sol–gel method is alternative to modify this parameter and therefore photocatalytic activity [14]. Fig. 3 shows the E_{phot} for the TiO_2-P-200 °C, this catalyst showed the higher E_g value (3.95 eV), a small particle size (12 nm) and an anatase phase with a minor rutile proportion (Fig. 1) (Table 1). The FT-IR spectra for the four sol–gel catalysts show the following bands: OH group vibration with the Ti atoms at 3641 cm^{-1}; enlargement vibration of the bond in the Ti–O–Ti structure at 1122 cm^{-1}; OH vibrational flexion at 1630 cm^{-1} (typical band of the physisorbed water in the material), which is of greater interest for photocatalytic purposes.

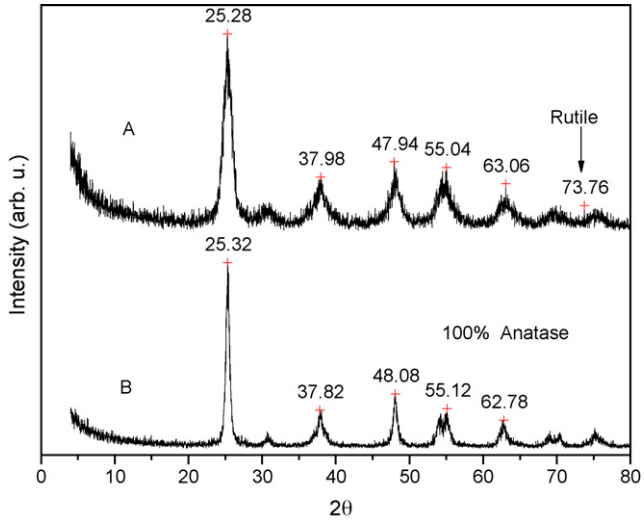

Fig. 1. XRD pattern for TiO_2-P-200 °C (A) and TiO_2-E-500 °C (B) sol–gel catalyst.

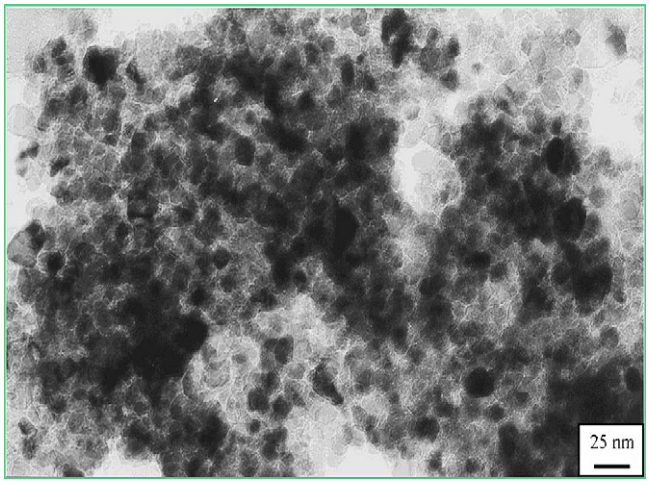

Fig. 2. TEM-micrograph for TiO_2-E-200 °C sol–gel catalyst.

Table 1
Characterization of TiO_2 sol–gel catalysts

Catalysts	Surface area ($m^2 g^{-1}$)	Pore volume (cm^3/g^{-1})	Mean pore diameter (Å)	Crystal size (nm)	Photon energy, $h\nu$ (E_g)
TiO_2-P-200 °C	189	0.17	36	12	3.95
TiO_2-P-500 °C	60	0.11	74	33	3.15
TiO_2-E-200 °C	212	0.25	48	10	3.05
TiO_2-E-500 °C	72	0.16	91	30	3.1

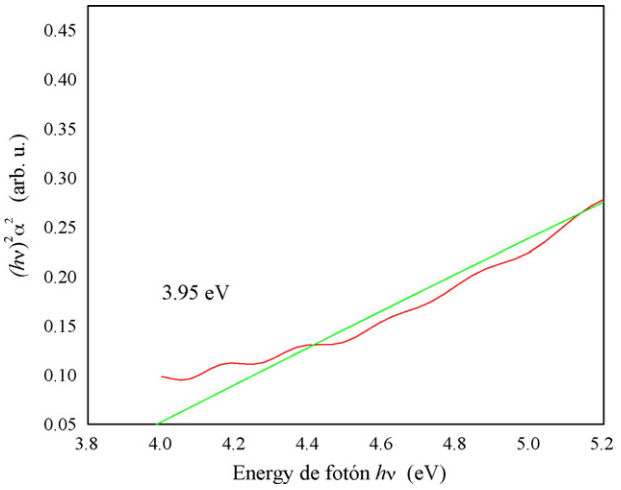

Fig. 3. Plot of $(h\nu)^2\ \alpha^2$ vs. E_{phot} for TiO_2-P-200 °C sol–gel catalyst.

Through the application of the sol–gel method and thermal treatments, it was possible to modify the textural and morphologic properties of synthesized catalysts, for instance, in two of them, which were activated at a low temperature (200 °C), the minor particle size (10 and 12 nm), stabilization of the anatase phase and changes on its bandgap (E_{phot}), were obtained. The properties mentioned above could be related to the activity and selectivity showed by the sol–gel catalysts, since to a high NO concentration (50 ppm), the NO decomposition was higher than 80%. Particularly, the TiO_2-E-200 °C showed a high NO decomposition (>80%) during the first 30 min, as well as a low selectivity towards NO_2 formation (Figs. 4 and 5). The TiO_2-E-200 °C-photocatalytic activity could be related to the particle size and the anatase phase. Both characteristics could have exerted an effect on the forbidden-energy bandgap (3.95 eV), which can improve the photoinduced electron transfer to adsorbed NO as a result of the migration of electrons and holes to the surface of the bulk TiO_2 sol–gel [15].

With respect to selectivity towards the NO_2 formation in sol–gel catalysts activated at a high temperature (TiO_2-P-500 °C and TiO_2-E-500 °C), it could be due to surface defect sites since

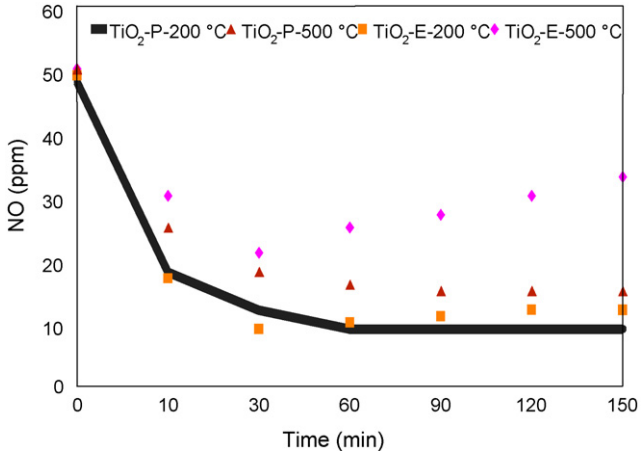

Fig. 4. Dependence of NO concentrations on the time in sol–gel catalyst.

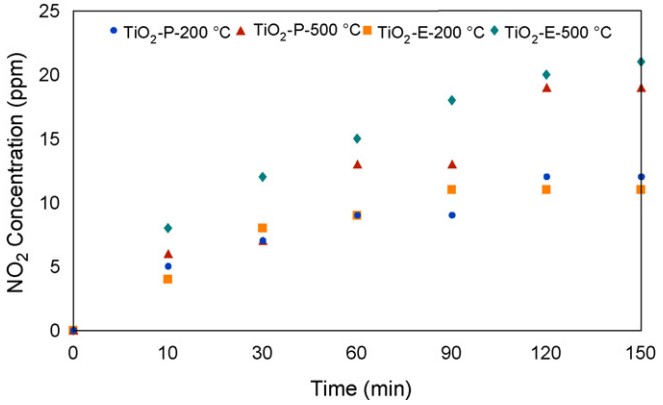

Fig. 5. Selectivity to NO_2 formation in sol–gel catalyst.

these are the precursors of further dissociative reactions between the adsorbed O_2 and of bulk oxygen vacancies, where the O species may attack adsorbed NO to yield NO_2 at the proposed reaction conditions.

4. Conclusions

The handling of the sol–gel variables permitted the synthesis of titania nanoparticles with improved textural and morphologic properties such as: high specific area, purity, stabilization of the anatase phase and modification of bandgap energy (E_g), especially those that were treated at a low temperature (200 °C). These properties offer a high photocatalytic activity over NO decomposition and a minor NO_2 selective formation even at a high NO concentration (50 ppm). The sol–gel catalysts activated at a low temperature can be considered as a good option for application to reduce the NO indoors and under atmospheric conditions with UV light assistance.

Acknowledgments

We are indebted to the IMP-Molecular Engineering Program and CONACyT for its financial support. The authors want to thank Technician Rufino Velázquez Lara for his assistance and technical support in this work.

References

[1] N.L. Stock, J. Séller, K. Vinodgal, P.V. Kamat, Environ. Sci. Technol. 34 (2000) 1747.
[2] F.D. Ollis, H. Al-Ekabi, Photocatalytic Purification and Treatment of Water and Air, Elsevier Science, Amsterdam, 1993.
[3] M.A. Fox, M.T. Dulay, Chem. Rev. 93 (1993) 54.
[4] J. Zang, T. Ayusawa, M. Minagawa, K. Kinugawa, M. Matsuoka, M. Anpo, J. Catal. 198 (2001) 1.
[5] A. Fujishima, K. Hashimoto, T. Watanabe, TiO_2 Photocatalysis Fundamental Applications, Published by BKC, Inc., Tokyo, Japan, 1999.
[6] A. Fujishima, K. Hashimoto, Y. Kubota, J. Surf. Sci. Soc. Jpn. 16 (1995) 188.
[7] X. Bokhimi, A. Morales, O. Novaro, T. López, E. Sánchez, R. Gomez, J. Mater. Res. 10 (1995) 2778.
[8] X. Bokhimi, O. Novaro, R.D. Gonzalez, T. López, O. Chimal, M. Asomoza, R. Gómez, J. Solid State Chem. 144 (1999) 349.

[9] J. Yu, X. Zhao, Mater. Res. Bull. 36 (2001) 97.
[10] K. Wark, C.F. Warner, Contaminación del Aire, Origen y Control, ed. Limusa 5a Edición, México, 1995, pp. 44–82.
[11] J. Pasel, V. Speer, C. Albrecht, F. Richter, H. Papp, Appl. Catal. B: Environ. 25 (2000) 105.
[12] E. Sanchez, Y. Lopez, Mater. Lett. 25 (1995) 271–275.
[13] K.M. Reddy, S.V. Manorama, A.R. Reddy, Mater. Chem. Phys. 78 (2002) 239–245.
[14] J. Yu, X. Zhao, Q. Zhao, Mater. Chem. Phys. 69 (2001) 25.
[15] A.L. Linsebigler, G. Lu, J.T. Yates Jr., Chem. Rev. 95 (1995) 735–758.